Influence of Lattice Anharmonicity on the Longitudinal Optic Modes of Cubic Ionic Solids*

R. P. LOWNDES†
Spectroscopy Laboratory, Research Laboratory of Electronics, Massachusetts Institute of Technology, Cambridge, Massachusetts‡ 02139

(Received 15 August 1969)

The determination of the $k\approx0$ longitudinal-optic-mode frequencies and lifetimes from the dielectric $[\epsilon(\omega)]$ and inverse dielectric $[\eta(\omega)]$ response functions of simple cubic solids is discussed. Experimental results of the temperature dependence, over the range 5–400°K, of the $k\approx0$ LO frequencies and lifetimes of 18 alkali and thallium halides are given, as determined from Kramers-Kronig analyses of near-normal-incidence single-crystal reflectance data and from small-grazing-angle reflectance data from thin films on conducting substrates. In addition, the pressure dependence up to 5 kbars at 290°K of the LO frequencies of RbI, CsBr, and CsI is reported. At 5°K the Lyddane-Sachs-Teller relation holds within ±3% for all the salts, and even at 290°K the relation is obeyed within ±10%. The temperature and pressure results are used to determine the self-energies and Grüneisen constants for the LO modes. At room temperature, the self-energy contributions are positive for those salts crystallizing in the NaCl structure and negative for those salts taking the CsCl structure. This is interpreted in terms of competing three-phonon and four-phonon decay and scattering processes.

1. INTRODUCTION

IF the lattice potential energy of a crystal were perfectly harmonic, the phonon frequencies would be independent of both temperature and volume. Evidence of the actual anharmonic lattice potential present in real materials like the alkali halides is readily available from a variety of experimental investigations, for instance, from the observed temperature[1,2] and volume[3,4] dependence of the frequencies and lifetimes of the $k\approx0$ transverse optic modes of these salts. The investigations conducted so far have revealed only a small intrinsic temperature dependence of the $k\approx0$ transverse optic modes compared to their intrinsic volume dependence.[4] To date, few investigations of any kind of the $k\approx0$ longitudinal optic modes of the alkali halides have been made.[5] In this paper we report on the detailed temperature dependence of the $k\approx0$ longitudinal modes for some alkali and thallium halides and also on the pressure dependence of these modes for RbI, CsBr, and CsI, The results are used to separate those effects of anharmonicity which are explicitly temperature dependent from those which are explicitly volume dependent. The former contributions are discussed in terms of the self-energies of the $k\approx0$ longitudinal optic modes and the latter contributions are discussed in relation to the Grüneisen constants of these modes.

2. DETERMINATION OF LO FREQUENCIES AND LIFETIMES

Although the transverse nature of electromagnetic waves prohibits their interaction with longitudinal optic phonons in infinite media, Berreman[5] has shown for cubic systems and Lowndes *et al.*[6] have shown for anisotropic systems that infrared-absorption measurements can, for suitable sample-radiation geometries, be used to measure the frequency of $k\approx0$ longitudinal optic phonons when thin strata (noninfinite) samples are used. We discuss now the significant properties of the dielectric response functions for cubic systems by which a determination of the $k\approx0$ LO phonon frequencies and lifetimes is achieved from infrared spectropic measurements.

For cubic systems, the three principal components of the dielectric tensor are degenerate. In the following discussion it is assumed that the applied electromagnetic fields are small compared with the internal crystal fields, and hence we may retain only a linear relation between the dielectric displacement D and the electric field E, which may be written either as

$$D(\omega)=\epsilon(\omega)E(\omega)\,, \tag{1}$$

where $\epsilon(\omega)$ is a frequency-dependent complex dielectric constant, or as

$$E(\omega)=\eta(\omega)D(\omega)\,, \tag{2}$$

where

$$\eta(\omega)\equiv1/\epsilon(\omega)\,. \tag{3}$$

The choice of equation depends on the type of vibration under consideration and is determined by whether $D(\omega)$ or $E(\omega)$ drives the system. In dealing with long-wavelength transverse optic waves the electric field $E(\omega)$ drives the system, and hence the use of the dielectric response function $\epsilon(\omega)$ in Eq. (1) is the more appro-

* Work performed in part at Queen Mary College, University of London.

† Present address: Physics Department, Northeastern University, Boston, Mass. 02115.

‡ Work supported in part by the Joint Services Electronics Program under Contract No. DA 28-043-AMC 02536(E).

[1] G. O. Jones, D. H. Martin, P. A. Mawer, and C. H. Perry, Proc. Roy. Soc. (London) **A261**, 10 (1961).

[2] R. P. Lowndes and D. H. Martin, Proc. Roy. Soc. (London) **A308**, 473 (1969).

[3] S. S. Mitra, C. Postmus, and J. R. Ferraro, Phys. Rev. Letters **18**, 455 (1967).

[4] C. Postmus, J. R. Ferraro, and S. S. Mitra, Phys. Rev. **174**, 983 (1968).

[5] D. W. Berreman, Phys. Rev. **130**, 2193 (1963).

[6] R. P. Lowndes, J. F. Parrish, and C. H. Perry, Phys. Rev. **182**, 913 (1969).

priate response function in this case. In dealing with long-wavelength longitudinal optic modes, it is the dielectric displacement $D(\omega)$ which drives the system and the inverse dielectric response function $\eta(\omega)$ is now more appropriate.[7]

Both $\epsilon(\omega)$ and $\eta(\omega)$ will, in general, be complex and for $\epsilon(\omega)$ and $\eta(\omega)$ to follow causal behavior requires that $\epsilon(\omega)=-\epsilon^*(\omega)$ and $\eta(\omega)=-\eta^*(\omega)$, where the asterisk indicates the complex conjugate. Because of causality, the poles and zeros of $\epsilon(\omega)$ and $\eta(\omega)$ will be either above the real axis or below it[8] depending on which sign convention is used to describe time periodic functions. Since the dielectric constant for the compounds considered here is a scalar quantity, causality further requires that the poles and zeros of $\epsilon(\omega)$ and $\eta(\omega)$ be symmetrically distributed about the imaginary axis of the ω plane[8] (this would also be true for a second-rank tensor dielectric response function). It is clear that a pole of $\epsilon(\omega)$ and a zero of $\eta(\omega)$ will occur whenever a frequency ω_T occurs for which $E(\omega_T)=0$ and $D(\omega_T)\neq 0$, that is for a transverse optic frequency; similarly, a zero of $\epsilon(\omega)$ and a pole of $\eta(\omega)$ will occur for a frequency ω_L at which $E(\omega_L)\neq 0$ and $D(\omega_L)=0$, that is at a longitudinal optic frequency.

We are primarily concerned here with the response function $\eta(\omega)$. The most general form for $\eta(\omega)$ for a system of N oscillators may be written as[9]

$$\eta(\omega)=\prod_{j=1}^{N}\eta_\infty\frac{(\omega-\omega_{Zj})(\omega-(-\omega_{Zj}{}^*))}{(\omega-\omega_{Pj})(\omega-(-\omega_{Pj}{}^*))}, \tag{4}$$

where ω is the applied field frequency and ω_Z and ω_P represent, respectively, the complex frequencies of zero's and poles in $\eta(\omega)$; η_∞ is a constant used to collectively describe the poles and zero's in $\eta(\omega)$ due to intrinsic electronic transitions and is defined as $\eta_\infty=1/\epsilon_\infty$, where ϵ_∞ is the high-frequency dielectric constant. Because of the consequences of anharmonic interactions in real crystals, the locations of the transverse and longitudinal-optic-mode frequencies and their associated damping can be defined in a somewhat arbitrary manner and we do so here in the following way:

$$\omega_{Tj}{}^2=(\omega_{Zj}{}')^2+(\omega_{Zj}{}'')^2, \tag{5a}$$

$$\omega_{Lj}{}^2=(\omega_{Pj}{}')^2+(\omega_{Pj}{}'')^2, \tag{5b}$$

$$\Gamma_{Tj}=-2\omega_{Zj}{}'', \tag{5c}$$

$$\Gamma_{Lj}=-2\omega_{Pj}{}''. \tag{5d}$$

Equation (4) then reduces to

$$\eta(\omega)=\prod_{j=1}^{N}\eta_\infty\frac{\omega_{Tj}{}^2-\omega^2-i\Gamma_{Tj}\omega}{\omega_{Lj}{}^2-\omega^2-i\Gamma_{Lj}\omega}. \tag{6}$$

The fundamental goal in an experimental analysis of $\epsilon(\omega)$ or $\eta(\omega)$ is to determine the location of the frequencies ω_{Tj} and ω_{Lj} and to determine the magnitude of the damping constants Γ_{Tj} and Γ_{Lj}. We consider here the case for $N=2$ in Eq. (6). [This, in fact, provides a close approximation for the $\eta(\omega)$ response functions for most of the salts considered later.] In this case, $\eta''(\omega)$, the imaginary part of $\eta(\omega)$, is given by

$$\eta''(\omega)=\frac{\eta_\infty}{\omega_L{}^4}\left[\frac{(\Gamma_L-\Gamma_T)\omega^3+(\Gamma_T\omega_L{}^2-\Gamma_L\omega_T{}^2)\omega}{(1-\omega^2/\omega_L{}^2)^2+\gamma^2\omega^2/\omega_L{}^4}\right]. \tag{7}$$

It is well known that a maximum in the $\omega\epsilon''$ or ϵ''/ω and $|\omega\eta''|$ or $|\eta''/\omega|$ for a classical-oscillator dielectric response function (i.e., where $\Gamma_L=\Gamma_T$) will, respectively, exactly locate ω_T and ω_L. For real crystals, however, the classical-oscillator model does not hold (since, for instance, $\Gamma_L\neq\Gamma_T$) and so we have

$$\left[\frac{\partial(\omega\eta'')}{\partial\omega}\right]_{\omega=\omega_L}=-\frac{2\eta_\infty\omega_L(\Gamma_L-\Gamma_T)}{\Gamma_L{}^2}\neq 0, \tag{8}$$

$$\left[\frac{\partial\eta''/\omega}{\partial\omega}\right]_{\omega=\omega_L}=\frac{2\eta_\infty\omega_L}{\Gamma_L{}^2}\left(\frac{\Gamma_T\omega_L{}^2}{\omega_L{}^4}-\frac{\Gamma_L\omega_T{}^2}{\omega_L{}^4}\right)\neq 0. \tag{9}$$

If a plane electromagnetic wave is to propagate through the system, then we must have $\epsilon''(\omega)\geq 0$ and $\eta''(\omega)\leq 0$, which leads to the conclusion that

$$\Gamma_L-\Gamma_T\geq 0 \quad \text{and} \quad \Gamma_T\omega_L{}^2-\Gamma_L\omega_T{}^2\geq 0. \tag{10}$$

Equations (8)–(10) therefore reveal that the turning point in $[\partial\omega\eta''/\partial\omega]$ occurs at a frequency below ω_L and that the turning point in $[(\partial\eta''/\omega)/\partial\omega]$ occurs at a frequency above ω_L.[10] For the compounds investigated here the turning points in these two functions occur within 1 cm^{-1} of each other, and so either of the functions may be used to conveniently locate ω_L. Exactly similar arguments can be used to define a frequency interval in which ω_T must exist from $\omega\epsilon''$ and ϵ''/ω functions.[10]

For systems where $(\Gamma_L/\omega_L)^2\ll 1$, as is the case for nearly all the salts considered here, the width at half height of the functions $\omega\eta''$ and η''/ω are given, respectively, by $\Delta\omega_1$ and $\Delta\omega_2$ as

$$\Delta\omega_1\approx\Gamma_L\left[1-\frac{\Gamma_L}{2\omega_L}Z_1+\frac{1}{8}\frac{\Gamma_L{}^2}{\omega_L{}^2}Z_1{}^2\cdots\right], \tag{11a}$$

[7] A. S. Barker, in *Ferroelectricity*, edited by E. F. Weller (Elsevier Publishing Co., Amsterdam, 1967).

[8] A. S. Davidov, in *Quantum Mechanics*, translated and edited by D. ter Haar (Addison-Wesley Publishing Co., New York, 1965), Sec. 112.

[9] D. W. Berreman and F. C. Unterwald, Phys. Rev. **174**, 791 (1968).

[10] J. F. Parrish, MIT Quarterly Progress Report **90**, 37 (1968).

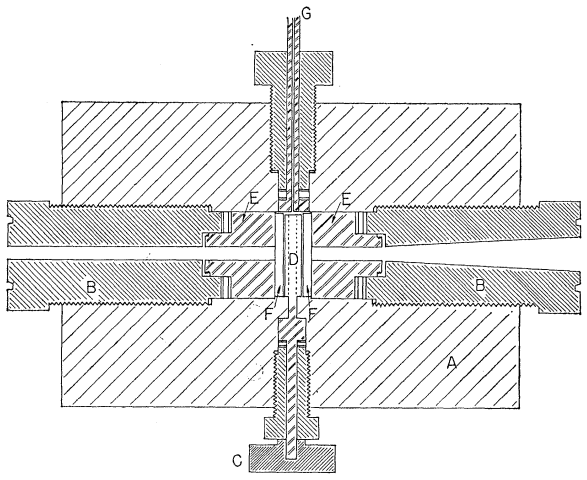

FIG. 1. Far-infrared high-pressure cell. A, cell body; B, window plugs; C, specimen changer; D, specimen holder; E, window mount; F, crystal quartz window; G, high-pressure transmission-line inlet.

where

$$Z_1=\frac{1+\omega_T^2/\omega_L^2-2\Gamma_T/\Gamma_L}{1-\omega_T^2/\omega_L^2}$$

and

$$\Delta\omega_2\approx\Gamma_L\left[1-\frac{\Gamma_L}{2\omega_L}Z_2+\frac{\Gamma_L^2}{16\omega_L^2}Z_2^2\cdots\right], \quad (11b)$$

where

$$Z_2=\frac{3-\omega_T^2/\omega_L^2-2\Gamma_T/\Gamma_L}{1-\omega_T^2/\omega_L^2}.$$

If $\Gamma_T=\Gamma_L$, as for the classical oscillator, then Eqs. (11) reduce to the classical-oscillator results (i.e., $\Gamma_L=\Gamma_T$):

$$\Delta\omega_1\approx\Gamma_L(1+\Gamma_L/2\omega_L)$$

and

$$\Delta\omega_2\approx\Gamma_L(1-\Gamma_L/2\omega_L).$$

In a similar way, the width at half-height of the functions $\omega\epsilon''$ and ϵ''/ω are given, respectively, by $\Delta\omega_3$ and $\Delta\omega_4$ as

$$\Delta\omega_3\approx\Gamma_T\left(1-\frac{\Gamma_T}{2\omega_T}Z_1+\frac{1}{8}\frac{\Gamma_T^2}{\omega_T^2}Z_1^2\cdots\right), \quad (12a)$$

$$\Delta\omega_4\approx\Gamma_T\left(1-\frac{\Gamma_T}{2\omega_T}Z_2+\frac{1}{16}\frac{\Gamma_T^2}{\omega_T^2}Z_2^2\cdots\right). \quad (12b)$$

We find that $Z_1\approx1$ and $Z_2\approx2$ for the salts investigated here, so that only the first two terms in these expansions need be considered to obtain a good estimate of the values Γ_L and Γ_T. By separately determining ϵ'' and η'' as a function of frequency, therefore, an iterative procedure involving, say, either Eqs. (11) or (12) can be used to determine Γ_L and Γ_T. In the present work such an iterative procedure in many cases provided adjustments of less than 5% to the values of Γ_L determined as the value of $\Delta\omega_1$ or $\Delta\omega_2$. Since for the main part such adjustments were less than the experimental error, the values of Γ_L were taken directly as the half-height widths $\Delta\omega_1$ or $\Delta\omega_2$.

The frequency dependence of η'' or ϵ'' is readily obtained from a Kramers-Kronig analysis of reflectance measurements using the Fresnel formulas appropriate for a crystal aligned with the desired axis precisely parallel to the incident electric field and perpendicular to the plane of incidence. However, as Berreman[5] first demonstrated, the longitudinal optic modes can be more directly studied from thin-film measurements. The π polarized reflectance component R_π of a thin film on a conducting substrate is given to a good approximation by

$$1-R_\pi=-A\omega\eta''$$

with

$$A=(4d/c)(\sin^2\theta/\cos\theta),$$

where θ is the angle of incidence, c is the velocity of light, and d is the film thickness. Since A will be constant in any one experiment, it is clear from the previous discussion that ω_L will be located by the frequency position of the maximum of $(1-R_\pi)/\omega^2$, and that Γ_L will be determined to a good approximation by measuring the width of the curve of $(1-R_\pi)/\omega^2$ at $R_\pi=\frac{1}{2}(1+R_\pi{}^L)$, where $R_\pi{}^L$ is the magnitude of R_π at $\omega=\omega_L$.

3. EXPERIMENT

The infrared spectroscopic measurements to determine the dispersion of η'' in the region of ω_L were recorded partly on an $f2$ single-pass grating instrument of the Ebert type and partly with an R.I.I.C. (London) 520 Fourier spectrophotometer used in conjunction with a liquid-helium-cooled Ga-doped germanium bolometer.

The frequency dependence of η'' was determined for most salts from a measurement of R_π (angle of incidence $\approx80°$) for thin films evaporated on aluminized mirrors. Many of the compounds were hygroscopic to some extent. An evaporation gun was therefore incorporated into the low-temperature cryostat and the thin films of these more hygroscopic compounds were prepared *in situ* without exposing them to the atmosphere. For a few compounds, $\eta''(\omega)$ was also determined from Kramers-Kronig analyses of reflectance data taken at near normal incidence (angle of incidence $\approx7\frac{1}{2}°$) from single-crystal samples.

High-pressure spectroscopic studies of ω_L were made using the far infrared pressure bomb shown in Fig. 1. The pressure bomb is capable of operating up to 10 kbar using either dry nitrogen or argon gas as the compression medium. In the present experiments the pressure was delivered to the bomb by a Harts compressor. The radiation ports in the bomb were 1 cm in diam and consisted of two 5-cm-diam crystal quartz blanks,

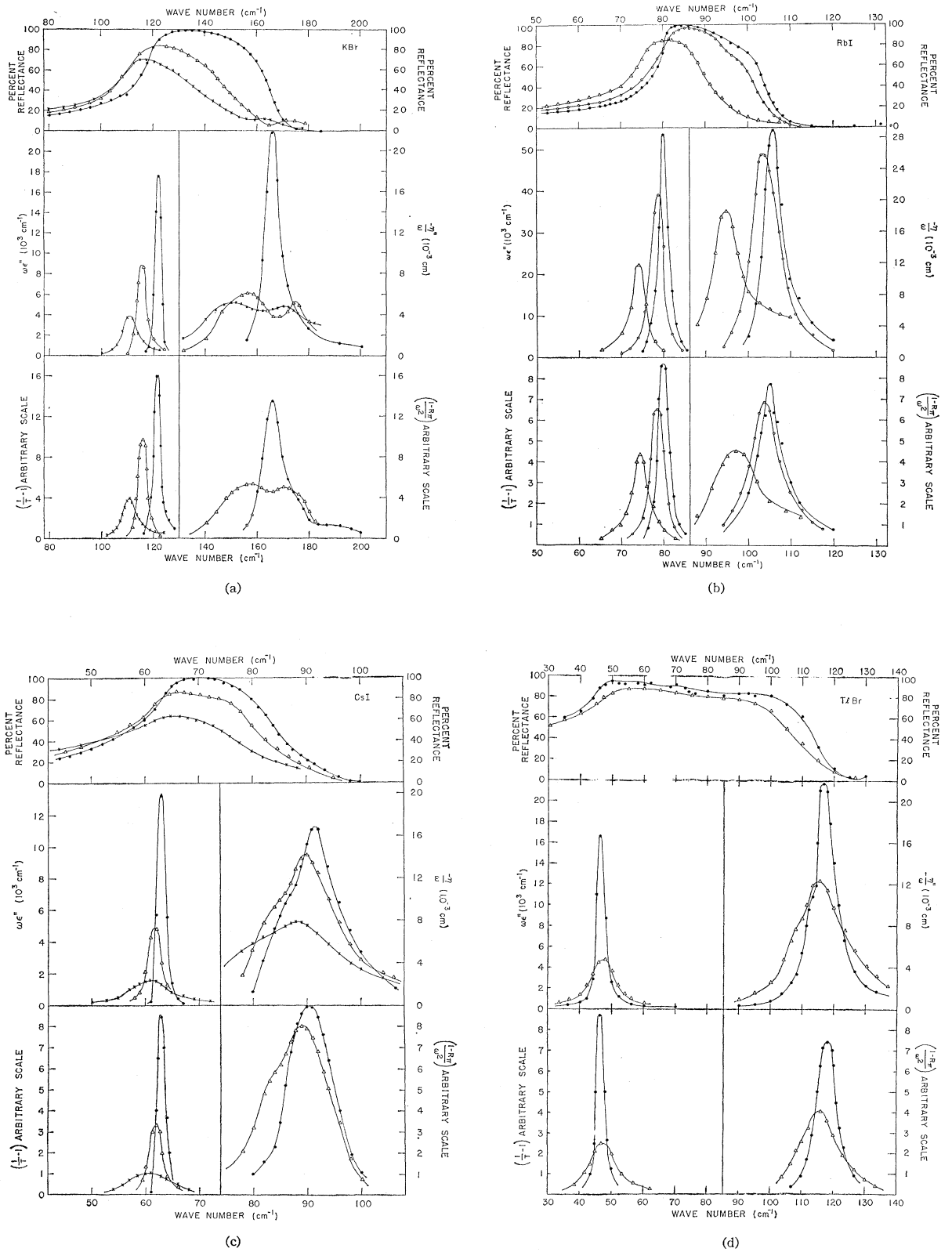

FIG. 2. Temperature dependence of the reflectance and dielectric functions $\omega\epsilon''$ and $-\eta''/\omega$ for (a) KBr, (b) RbI, (c) CsI, (d) TlBr. ●—● 5°K, ○—○ 80°K, △—△ 290°K, ×—× 400°K.

TABLE I. Values of ω_L, in cm^{-1}, as determined from Kramers-Kronig (KK) analyses of reflectance data, from small-grazing-angle thin-film reflectance data (film) and from the Lyddane-Sachs-Teller (LST) relation. The neutron measurements are taken from Refs. 13–16. An asterisk indicates the frequency location of side bands in the close vicinity of ω_L. The measuring accuracy is ± 0.5 cm^{-1}.

	5°K			80°K		90°K	200°K		290°K			400°K	
	LST	KK	Film	KK	Film	Neutron	KK	Film	LST	KK	Film	KK	Film
LiF	671	673	673	673	673		672	672	661	671	670		
LiCl	435		435		433			429	421		425		
NaF	431		426		426			424			421.5		
NaCl	271		266		264	264		264	261		250*, 263		
NaBr	216		212		210			206	208		202		
NaI	181		174		172	172			180		164		
KF	335		335						335		330		
KCl	212	212, 228*	212, 226*	211.5, 228*	210, 224*		205, 223*	204, 222*	211	198.5, 218*	198, 220*		
KBr	170	166	166	164	165	167	161	161	165	157, 175*	157, 173*	150, 170*	157 171
KI	145	143.5	143	141	141	142	134.5	134	142	129, 145	127, 145*		
RbF	286		290						290		285		
RbCl	181		182, 200*		180, 200*			173, 195*	175		167, 191*		
RbBr	130		134		133			130	126		128		
RbI	108	105.5	105.5	104	104		100	101	104	95	97.5	86	88
CsCl	168		163		162.5			161.5	162		160		158
CsBr	115		115		114			113.5	114		113		112
CsI	94	91.5	91.5	91.5	91		91	91	91	90.5	90.5	89	89
TlBr	118	117	118	116	117.5	112	116	116	117	116	115.5	115	114

lapped optically flat and parallel to better than 300 Å with the martensitic steel window mounts E. An elliptical specimen holder D containing a sample port and a blank reference port was manually operated externally to the bomb by rotating the control changer C, thus permitting both sample and reference spectra to be recorded without changing the internal environmental condition of the bomb. In studying the pressure dependence of ω_L, large incident-angle transmission measurements on thin films on lossless substrates were used.[5] The use of the radiation guide and cone in the support window plugs B ensured that the radiation, through repeated reflection, would strike the samples mounted in the plane of D (perpendicular to the figure plane) at large angles of incidence.

4. RESULTS

Figure 2 shows the measured reflectance at near normal incidence from bulk samples of KBr, RbI, CsI, and TlBr at different temperatures and compares the frequency dependence of η''/ω determined from Kramers-Kronig analyses of this reflectance data with the frequency dependence of $(1-R_\pi)/\omega^2$ determined from the small-grazing-angle reflectance of thin films. Also shown for completeness are the functions $\omega\epsilon''$,

TABLE II. Values of Γ_L/ω_L determined from KK analyses and from thin-film measurements.

	5°K			80°K		200°K		290°K		
	KK	Film	Γ_L/Γ_T	KK	Film	KK	Film	KK	Film	Γ_L/Γ_T
LiF	0.040	0.045	4.2	0.060	0.060	0.075	0.080	0.090	0.100	3.9
LiCl		0.130	4.0		0.160		0.260		0.340	4.2
NaF		0.050	3.2		0.070		0.120		0.170	4.2
NaCl	0.045	0.050	4.9		0.070					
NaBr		0.070	4.4		0.110		0.170		0.220	5.3
NaI		0.090	4.2		0.120		0.180		0.230	4.0
KF		0.090	2.5							
KBr	0.035	0.050	9.0	0.055	0.070					
KI	0.050	0.055	4.2	0.057	0.080					
RbF		0.080	3.6							
RbCl		0.060	4.2		0.075		0.110		0.160	5.7
RbBr		0.070	6.8		0.105		0.140		0.170	7.3
RbI	0.060	0.075	6.5	0.085	0.100	0.105	0.125	0.125	0.150	5.2
CsCl		0.100	4.5		0.120		0.165		0.205	5.4
CsBr		0.055	4.3		0.065		0.080		0.100	2.8
CsI	0.115	0.065	5.6	0.125	0.090	0.140	0.120	0.170	0.160	5.5
TlBr	0.060	0.070	2.0	0.075	0.080	0.125	0.120	0.170	0.150	2.6

determined from bulk-crystal reflectance data, and the function $(1/T-1)$ determined from the transmittance T of thin films on lossless substrates (polystyrene or mica) for near-normal-incident radiation. The figures reveal that the location of ω_L, determined from the frequency position of the turning point in η''/ω, are in close agreement for the two methods of determination. In addition, the line shape, as defined by the profiles of η''/ω are in reasonable agreement for both types of measurement.

Table I summarizes values of ω_L for eighteen salts in the temperature range 5–400°K determined from both types of experimental measurement. Where there is overlap between the two measuring techniques, it can be seen that there is over-all agreement between the frequencies to better than 1%. The spectra for several of the compounds showed strong subsidiary bands in the close proximity of the fundamental longitudinal optic modes, as illustrated in Fig. 3 for KBr, and the frequencies of these subsidiary bands are indicated in the table by an asterisk. These side bands are thought to be associated with two phonon-decay and scattering processes.

Table II lists the observed values of Γ_L/ω_L determined from the thin-film and single-crystal measurements. For those salts where the line profile close to ω_L contains a distinct double peak it is clear that the simplified analysis of Sec. 2 to obtain Γ_L does not apply. No values of Γ_L/ω_L have therefore been included in Table II for such cases. Data are not included for KF and RbF at other than 5°K, partly because the widths at half-height were too large at higher temperatures for the approximations contained in Sec. 2 to hold and partly because of the comparatively large error involved in measuring these widths. It is not clear whether these large values of Γ_L/ω_L reflect a genuine short lifetime for these LO phonons or whether it is to some extent an artifact due to the less pure starting material used in the preparation of these films. As Table II shows, the lifetimes of the $k\approx 0$ LO phonons in the alkali halides are significantly shorter than those of the $k\approx 0$ TO phonons.

Figure 3 shows the pressure dependence of the $k\approx 0$ LO frequencies of RbI and CsI for pressures up to 5 kbar at 290°K. Even though the pressure-induced shifts were small, because of the point-by-point measuring technique used and the lack of any observable hysteresis during the pressurizing cycle, the measurements of $[\partial\omega/\partial P]_T$ are thought to have an accuracy within ±15%.

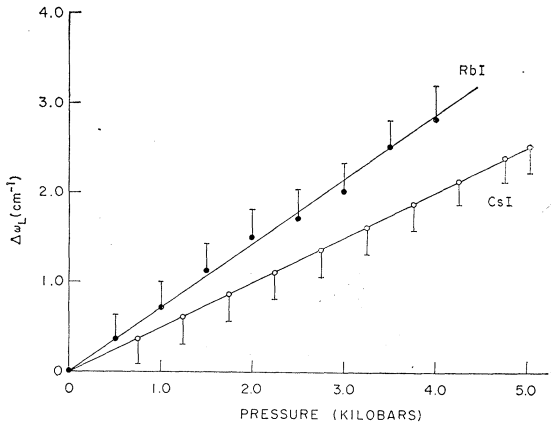

FIG. 3. Measured pressure dependence of ω_L for RbI and CsI.

5. DISCUSSION

A. Lyddane-Sachs-Teller Relation

On the basis of a simple microscopic model of the dielectric properties of cubic diatomic ionic solids, Lyddane, Sachs, and Teller[11] obtained the relation

$$\omega_L^2=\omega_T^2(\epsilon_0/\epsilon_\infty).$$

The assumptions based in their derivation of this relation were that the equation of motion and polarization of the system vary linearly as the amplitude of the applied field and that the effective polarizing field at a lattice site depends on the macroscopic and Lorentz internal field. The relation is somewhat more general than was first implied, however, and it is readily shown that the relation follows from causal behavior provided the ϵ'' curve exhibits a δ function at ω_T. Cochran and Cowley[12] have shown that the relation holds in any crystallographic direction for crystals of any symmetry within the adiabatic, electrostatic, and harmonic approximation. The comparatively few measurements of ω_L for any solids have prevented any rigorous over-all assessment of the LST relation. Neutron scattering measurements have determined ω_L, for KBr,[13] NaI,[13] KI,[14] TlBr,[15] and NaCl[16] at 90°K, and some verifications have been made for piezoelectric crystals where the optic modes are simultaneously infrared and Raman active.[17] Using the recently reported values of ω_T, ϵ_0, and ϵ_∞ for the salts considered here,[2] values of ω_L have been calculated for temperatures of 5 and 290°K and these are listed in Table I. The results indicate that the LST relation holds to better than 3% at 5°K and is in reasonably good agreement even at 290°K, although discrepancies of as much as 10% were noted in some cases. The degree of agreement

[11] R. H. Lyddane, R. G. Sachs, and E. Teller, Phys. Rev. **59**, 673 (1941).
[12] W. Cochran and R. A. Cowley, J. Phys. Chem. Solids **23**, 447 (1962).
[13] A. D. Woods, B. N. Brockhouse, and R. A. Cowley, Phys. Rev. **131**, 1025 (1963).
[14] G. Dolling, R. A. Cowley, C. Schittenhelm, and I. M. Thorson, Phys. Rev. **147**, 577 (1966).
[15] E. R. Cowley and A. Okazaki, Proc. Roy. Soc. (London) **A300**, 45 (1967).
[16] G. Raunio, L. Almqvist, and R. Stedman, Phys. Rev. **178**, 1496 (1969).
[17] R. Loudon, Advan. Phys. **14**, 423 (1964).

TABLE III. Values of $(1/\omega)[\partial\omega/\partial P]_T$ and γ_L for RbI, CsBr, and CsI.

	β (10^{-12} cm^2 dyn^{-1})	ω_L (cm^{-1})	$(1/\omega_L)[\partial\omega_L/\partial P]_T$ (10^{-3} kbar^{-1})	γ_L
RbI	9.66	97.5	7.3	0.76
CsBr	6.69	113.0	4.2	0.63
CsI	8.40	90.5	5.7	0.68

at low temperatures is encouraging and provides some support for the use of the harmonic approximation in lattice dynamical calculations for these salts at temperatures close to 0°K.[18,19]

B. One-Phonon Longitudinal Optic Grüneisen Parameters

The temperature dependence of each phonon frequency in the Brillouin zone stems from the anharmonic terms in the lattice potential energy in two separate ways. First, due to the thermal expansion of the crystal, the interionic force constants are temperature dependent, thus creating a quasiharmonic shift of each phonon frequency as the temperature (i.e., volume) changes. Secondly, lattice anharmonicity allows interactions between phonons of different modes and these interactions will change the phonon energies and give them a finite lifetime. Since the probability of such interactions occurring depends on the phonon-occupation number, it is clear that both the phonon frequency and lifetime will have a temperature dependence which will take place even under constant volume.

We consider first the variations of ω_L with volume. Within the limits of a quasiharmonic-oscillator model, the volume dependence of the $k\approx 0$ longitudinal-optic-mode frequency is described by

$$\gamma_L=-\left[\frac{\partial \ln\omega_L}{\partial \ln V}\right]_T, \tag{13}$$

where γ_L is the characteristic Grüneisen parameter for the LO mode. The Grüneisen parameter can be conveniently determined experimentally from the relation

$$\gamma_L=\frac{1}{\beta\omega_L}\left[\frac{\partial\omega_L}{\partial P}\right]_T, \tag{14}$$

providing the compressibility β and the pressure coefficient under constant temperature of ω_L, $(1/\omega_L)[\partial\omega_L/\partial P]_T$, are known. Using the measured pressure dependence of ω_L reported here, the Grüneisen parameters for the $k\approx 0$ LO modes of RbI, CsBr, and CsI have been calculated and are listed in Table III.

An estimate of the Grüneisen constant γ_L for the remaining salts can be calculated from Szigeti's treatment of the static dielectric constant of cubic ionic crystals.[20] Szigeti obtains the following form for the static dielectric constant ϵ_0:

$$\epsilon_0=\epsilon_\infty+\tfrac{1}{3}(\epsilon_\infty+2)^2(4\pi e^{*2}/\mu v\omega_T^2)+G, \tag{15}$$

where ϵ_∞ is the high-frequency dielectric constant, e^* is the Szigeti effective charge,[21] and μ and v are the reduced mass and cell volume, respectively, for a cell unit. G is the pure anharmonic contribution to ϵ_0 and in Szigeti's treatment is assumed to be volume independent. From Sec. 4 it was clear that even at 290°K the LST relation held to a good approximation, so that Eq. (15) can be reduced to

$$\epsilon_0\approx\epsilon_\infty+\tfrac{1}{3}(\epsilon_\infty+2)^2\frac{4\pi e^{*2}}{\mu v\omega_L^2}\frac{\epsilon_0}{\epsilon_\infty}+G. \tag{16}$$

Differentiating Eq. (16) leads to

$$\gamma_L=-\left[\frac{\partial \ln\omega_L}{\partial \ln V}\right]_T=\frac{1}{2}\left[\frac{\partial \ln(\epsilon_0-\epsilon_\infty)}{\partial \ln V}\right]_T+\frac{1}{2}\left[\frac{\partial \ln\epsilon_\infty}{\partial \ln V}\right]_T$$
$$-\left[\frac{\partial \ln(\epsilon_\infty+2)}{\partial \ln V}\right]_T-\left[\frac{\partial \ln e^*}{\partial \ln V}\right]_T-\frac{1}{2}\left[\frac{\partial \ln\epsilon_0}{\partial \ln V}\right]_T+\tfrac{1}{2}. \tag{17}$$

The main difficulty in assessing γ_L from Eq. (17) is the calculation of the volume dependence of e^*. Born and Huang[22] have shown where distortion dipoles directed along anion-cation bonds are responsible for e^*, that

$$e^*-e=\tfrac{1}{3}N[m'(r_0)+2m(r_0)/r_0], \tag{18}$$

where N is the lattice coordination number, $m(r_0)$ is the distortion dipole between nearest neighbors at their equilibrium separation of r_0, and $m'(r_0)$ is the rate of change of $m(r_0)$ with lattice spacing. Mitskevich,[23] and Lowndes and Martin[2] have pointed out that the distortion-dipole moment in those alkali halides crystallizing in the NaCl structure contains a contribution arising from short-range Coulomb interactions between the hexadecapole moments of an ion and the monopole moments of its immediate neighbors, as well as the more established contribution from the short-range repulsive forces. It is found that[2,23] the total value of $m(r)$ is closely described by the form

$$m(r)=Ae^{-r/\rho},$$

where A is a constant, and r and ρ are the nearest-neighbor distance and the hardness parameter, respectively, as given by Born and Huang.[22] Assuming this to be generally true, Eq. (18) leads to

$$\frac{d\ln e^*}{d\ln V}=\frac{(e/e^*-1)(r_0/\rho^2-2/\rho-2/r_0)}{3(1/\rho-2/r_0)}. \tag{19}$$

[18] A. D. B. Woods, W. Cochran, and B. N. Brockhouse, Phys. Rev. **119**, 980 (1960).
[19] A. M. Karo and J. R. Hardy, Phys. Rev. **129**, 2024 (1963).
[20] B. Szigeti, Proc. Roy. Soc. (London) **A261**, 274 (1961).
[21] B. Szigeti, Trans. Faraday Soc. **45**, 155 (1949).
[22] M. Born and K. Huang, *Dynamical Theory of Crystal Lattices* (Oxford University Press, New York, 1954), pp. 26, 115.
[23] V. V. Mitskevich, Fiz. Tverd. Tela **5**, 3500 (1963) [English transl.: Soviet Phys.—Solid State **5**, 2568 (1964)].

Using the available data for e^*/e^2 and ρ and r_0 [22] together with available data for the volume dependence of ϵ_0 [24] and ϵ_∞ [25,26] allows an estimate of γ_L to be determined from Eq. (17). The values of γ_L so calculated are listed in Table IV and it can be seen that for those salts where γ_L was determined directly from experimental measurements there is reasonable agreement between the calculated and experimental values.

C. Self-Energy of the Londitudinal Optic Modes

We consider now the self-energy contribution to the over-all temperature dependence of the longitudinal optic modes. From Sec. 4 we may write the longitudinal optic frequency $\omega_L(T)$ in the form

$$\omega_L(T)=\omega_L(0)-\Delta\omega_L{}^E(T)-\Delta\omega_L{}^A(T), \qquad (20)$$

where $\omega_L(0)$ is the frequency at 0°K and $\Delta\omega_L{}^E(T)$ is the quasiharmonic shift due to thermal expansion and $\Delta\omega_L{}^A(T)$ is the self-energy shift. The quasiharmonic shift is defined as

$$\Delta\omega_L{}^E(T)=\omega_L(0)-\omega_L{}^E(T), \qquad (21)$$

where $\omega_L{}^E(T)$ is the characteristic frequency at temperature T that the solid would have if thermal-expansion processes only were responsible for the temperature dependence of ω_L. The quantity $\omega_L{}^E(T)$ can be calculated from

$$\ln\omega_L{}^E(T)=\ln\omega_L(0)-\gamma_L\int_0^T \alpha dT, \qquad (22)$$

where α is the volume coefficient of expansion. The self-energy shift is defined by

$$\Delta\omega_L{}^A(T)=\omega_L{}^E(T)-\omega_L(T), \qquad (23)$$

where $\omega_L{}^A(T)$ is the characteristic frequency at temperature T that would be recorded for a solid held under constant volume between $T=0$ and a temperature T.

Values of $\Delta\omega_L{}^E$ and $\Delta\omega_L{}^A$ determined from Eqs. (21) and (23) are summarized in Table III for the temperatures 80, 200, and 290°K. Values of α used in the calculation of the $\Delta\omega_L{}^E$ were taken from the literature.[27–31] A comparison of the magnitudes of $\Delta\omega_L{}^A$ at 290°K reveals that as we move from the heavier Rb halides to the lighter Li halides, the magnitude of the self-energy shift decreases significantly. In the case of the Rb and K halides, for example, the self-energy shift strongly dominates the shift due to thermal expansion while the reverse is true for the Na and Li halides. In the Cs halides the $\Delta\omega_L{}^E(290)$ also dominate the $\Delta\omega_L{}^A(290)$ but now these quantities are opposed in sign, unlike the results for the other alkali halides. The calculations show a reversal in the sign of the $\Delta\omega_L{}^A$ for the Cs halides at temperatures below 200°K. Similarly the calculations show the $\Delta\omega_L{}^A$ for the Na salts to be decreasing with increasing temperature so that the possibility exists that there could be a change in sign for these salts for the $\Delta\omega_L{}^A$ at temperatures higher than 290°K. However, because of the approximations made in the calculations of γ_L and because of the experimental uncertainties in the various quantities used in these calculations, the small magnitudes, of $\Delta\omega_L{}^A(290)$ determined here for LiF, NaF, NaCl, and CsCl do not decisively decide the sign of $\Delta\omega_L{}^A(290)$ for these salts; for the same reasons the calculations do not conclusively indicate that a reversal of sign for $\Delta\omega_L{}^A$ does take place for the Cs or Na salts.

TABLE IV. Calculated values of γ_L, $\Delta\omega_L{}^E$, and $\Delta\omega_L{}^A$ for several salts. An asterisk indicates an experimental value of γ_L. Frequencies are in cm^{-1}.

	γ_L	$\omega_L(0)$	$\Delta\omega_L{}^E$ (80)	$\Delta\omega_L{}^A$ (80)	$\Delta\omega_L{}^E$ (200)	$\Delta\omega_L{}^A$ (200)	$\Delta\omega_L{}^E$ (290)	$\Delta\omega_L{}^A$ (290)
LiF	0.22	673	0	0	1.0	0	2.2	0.8
NaF	0.67	426	0.2	0.3	2.3	0.3	4.3	0.2
NaCl	0.47	271	0.1	0.9	1.6	0.4	2.9	0.1
KCl	0.58	212	0.3	1.7	1.6	6.4	2.7	11.3
KBr	0.60	166	0.3	0.7	1.5	3.5	2.5	6.5
KI	0.51	143	0.2	1.8	1.2	7.8	2.1	13.9
RbCl	0.63	182	0.1	1.9	1.3	7.7	2.5	12.5
RbBr	0.58	134	0.2	0.8	1.2	2.8	2.0	4.0
RbI	0.52	105.5	0.3	1.2	0.9	3.6	1.5	6.5
RbI	0.76*	105.5	0.3	1.2	1.3	3.2	2.2	5.8
CsCl	0.64	163	0.6	−0.1	1.9	−0.4	3.8	−0.8
CsBr	0.57	115	0.3	0.7	1.3	0.2	2.2	−0.2
CsBr	0.63*	115	0.4	0.6	1.6	−0.1	2.5	−0.5
CsI	0.50	91.5	0.3	0.2	1.0	−0.5	1.6	−0.6
CsI	0.68*	91.5	0.4	0.1	1.3	−0.8	2.1	−1.1

A number of authors have deduced expressions for $\Delta\omega_L{}^A$ by perturbation theory (see review by Cowley[32]). Maradudin and Fein[33] have calculated the effect of cubic anharmonicity to second order and of quartic anharmonicity to first order in perturbation theory and they obtain an expression for $\Delta\omega_L{}^A$ of

$$\Delta\omega_L{}^A=+\frac{18}{\hbar^2}\sum_{\mathbf{q}_1\mathbf{q}_2 j_1 j_2}\left|V\begin{pmatrix}0 & \mathbf{q}_1 & \mathbf{q}_2\\ L & j_1 & j_2\end{pmatrix}\right|^2\left\{\frac{n_1+n_2+1}{\omega_1+\omega_2+\omega_L}+\frac{n_1+n_2+1}{\omega_1+\omega_2-\omega_L}+\frac{n_2-n_1}{\omega_1-\omega_2+\omega_L}+\frac{n_2-n_1}{\omega_1-\omega_2-\omega_L}\right\}$$
$$-\frac{12}{\hbar}\sum_{\mathbf{q}_1 j_1}V\begin{pmatrix}0 & 0 & \mathbf{q}_1 & -\mathbf{q}_1\\ L & L & j_1 & j_1\end{pmatrix}\{2n_1+1\}, \qquad (24)$$

[24] R. P. Lowndes and D. H. Martin, Proc. Roy. Soc. (London) (unpublished).
[25] E. Burstein and P. L. Smith, Phys. Rev. **74**, 229 (1948).
[26] H. Leibssle, Z. Krist. **114**, 457 (1960).
[27] F. A. Henglein, Z. Physik Chem. (Frankfort) **A115**, 91 (1925).
[28] B. Yates and C. H. Panter, Proc. Phys. Soc. (London) **80**, 373 (1962).
[29] G. K. White, Proc. Roy. Soc. (London) **A286**, 204 (1965).
[30] B. W. Jaffnes and B. Yates, Phil. Mag. **7**, 663 (1965).
[31] A. C. Bailey and B. Yates, Phil. Mag. **18**, 1241 (1968).
[32] R. A. Cowley, Rept. Progr. Phys. **31**, 123 (1968).
[33] A. A. Maradudin and A. E. Fein, Phys. Rev. **128**, 2589 (1962).

TABLE V. Comparison of values for $\Delta\omega_L{}^E$, $\Delta\omega_L{}^A$, and $\Delta\omega_L$ (in cm^{-1}) for KBr obtained from the present work with the shell-model calculations of Cowley.

	80°K	90°K	200°K		290°K	
	Present work	Cowley	Present work	Cowley	Present work	Cowley
$\Delta\omega_L{}^E$	0.3	3.4	1.5	6.5	2.5	9.2
$\Delta\omega_L{}^A$	1.7	−0.5	3.5	1.3	6.5	1.9
$\Delta\omega_L$	2.0	2.9	5.0	7.8	9.0	11.9

where $n_1=n(\mathbf{q}_1 j_1)$ is the thermal-expectation value for the occupation number of the phonon mode and $\omega_1=\omega(\mathbf{q}_1 j_1)$ is its frequency. The V coefficients derive from the lattice potential energy of deformation at constant volume, expanded in terms of the normal phonon coordinates. Equation (24) shows $\Delta\omega_L{}^A$ to be the sum of a positive term related to the cubic term in V and a term which derives from the quartic term in V which may be negative. The negative values found for $\Delta\omega_L{}^A$ at 290°K for the three Cs halides crystallizing in the CsCl structure would seem to indicate that the quartic contribution is indeed negative, and that in these cases this dominates the contribution from the cubic term. The small values of $\Delta\omega_L{}^A(290)$ determined for the Li and Na halides suggests that there is a near cancellation of the cubic and quartic terms in V at 290°K while the relatively large positive values of $\Delta\omega_L{}^A(290)$ determined for the K and Rb halides clearly indicate that the cubic terms in V provide the dominant contribution to $\Delta\omega_L{}^A$ for these salts. The reason for the dominance of the quartic contributions for compounds which have the CsCl structure is not entirely clear. Bosman and Havinga have suggested that the cubic terms could be of reduced significance in a CsCl structure because the higher-coordination number reduces the effect of fluctuations among the pairs of bonds formed by an ion with its neighbors.[34]

It is worth noting that $\Delta\omega_L{}^A(0)$ is not zero because anharmonic contributions exist in the presence of zero-point fluctuations. Extrapolations of the data in Tables I and IV indicate that $\Delta\omega_L{}^A(0)$ is positive for every compound with values ranging from near zero up to about 1% of $\omega_L{}^E$. This near-zero value of $\Delta\omega_L{}^A(0)$ may in fact be the reason why the observed values of $\omega_L(5)$ are nearly always 1–2% lower than the values calculated from the LST relation.

The general formula for the inverse lifetime given by Maradudin and Fein[33] can be reduced to describe the one-phonon main transition in the vicinity of ω_L as a damped Lorentzian resonance with a damping parameter Γ_L given by

$$\Gamma_L=\frac{18\pi}{\hbar^2}\sum_{\mathbf{q}_2 q_1 j_1 j_2}\left|V\begin{pmatrix}0 & q_1 & q_2\\ L & j_1 & j_2\end{pmatrix}\right|^2 \times[(n_1+n_2+1)\delta^S+(n_2-n_1)\delta^D], \quad (25)$$

where δ^S and δ^D are Dirac δ functions which are zero except for pairs of modes for which ω_L is near $(\omega_1+\omega_2)$ and $(\omega_2-\omega_1)$, respectively. Equation (25) reveals that $\Gamma_L\neq 0$ even at $T=0$°K. Extrapolations of the measured temperature dependence of Γ_L down to 5°K confirm this result. Equation (25) shows that the decay of the phonon at ω_L is proportional to the two-phonon density of states at ω_L. The strong attenuation at ω_L for many salts, especially for the double-peak profiles found in NaCl, KCl, KBr, KI, and RbCl, are therefore probably due to the presence of peaks in the two-phonon density of states at or near ω_L. The existence of a double peak feature near ω_L for KCl and RbCl at 5°K implies that this is due primarily to two-phonon summation processes.

A test of the observed temperature dependence of $\Delta\omega_L{}^A$ and Γ_L against the theoretical expressions in Eqs. (24) and (25) would require the evaluation of extensive summations over one- and two-phonon densities of states. Some simplification to the problem is achieved if we restrict our interest to temperatures higher (but not too high) than the effective Debye temperature for the salts, since at these temperatures the leading terms in expansions of the n_i give a linear temperature dependence of both $\Delta\omega_L{}^A$ and Γ_L. More detailed measurements of the temperature dependence of ω_L and Γ under constant pressure and constant volume are currently being made to temperatures well above the characteristic Debye temperatures of these salts in order to test these predictions. However, it is of interest to compare the values of $\Delta\omega_L{}^E$ and $\Delta\omega_L{}^A$ presented here with the shell-model calculations made by Cowley[35] for KBr. Table V shows that while the over-all temperature dependence of ω_L for KBr is in good agreement, the $\Delta\omega_L{}^E$ and $\Delta\omega_L{}^A$ obtained from the present work vary more slowly and more quickly with temperature, respectively, than indicated by Cowley's calculations.

6. SUMMARY

The measurement of the temperature and pressure dependence of the $k\approx 0$ LO modes of simple cubic ionic solids has allowed a first determination of the variation of ω_L at constant volume and of the magnitude of the self-energy contributions to these modes. The measurements reveal that the self-energies of these modes at 290°K can either enhance or oppose the temperature

[34] E. E. Havinga and A. J. Bosman, Phys. Rev. **140**, 292 (1965).

[35] R. A. Cowley, Advan. Phys. **12**, 421 (1963).

dependence of the modes arising from thermal expansion, depending on whether three-phonon processes due to cubic anharmonicity or four-phonon processes due to quartic anharmonicity give the overriding contribution to the self-energies. At 0°K only small residual self-energy contributions remain which amount to no more than 1% of the total LO phonon energies.

ACKNOWLEDGMENTS

It is a pleasure to acknowledge valuable discussions with Professor D. H. Martin, Professor C. H. Perry, and Dr. J. F. Parrish. It is also a pleasure to acknowledge the valuable technical assistance given by J. Weston in the design and construction of the high-pressure infrared bomb at Queen Mary College, London.

PHYSICAL REVIEW B VOLUME 1, NUMBER 6 15 MARCH 1970

Measurement of $(\partial P/\partial T)_V$ and Related Properties in Solidified Gases. III. Solid D_2†

DIETOLF RAMM* AND HORST MEYER
Department of Physics, Duke University, Durham, North Carolina 27706

AND

ROBERT L. MILLS
Los Alamos Scientific Laboratory, University of California, Los Alamos, New Mexico 87544

(Received 27 October 1969)

Measurements in solid D_2 of pressure changes with temperature and para concentration are reported, and related thermodynamic properties are calculated. The study covers both the hcp and cubic phases in the temperature range $0.4 \leqslant T \leqslant 4.2$ K and para concentration range $0.02 \leqslant c \leqslant 0.90$. The measurements were carried out with a capacitance strain gauge capable of resolving pressure changes of 2×10^{-5} bar. Two types of study were made. (a) The pressure changes accompanying the phase transition were determined as a function of c, and the hysteresis was studied as a function of the number of cyclings through the transition. (b) The quantity $(\partial P/\partial T)_V$ was obtained in the cubic and hcp phases as a function of T and c. The results were analyzed in terms of separate contributions from the lattice and from the rotation of the para-deuterium molecules (p-D_2, lowest rotational level $J=1$). The molecular rotation was assumed to be quenched by the electric quadrupole-quadrupole (EQQ) interaction, and all other effects such as those due to crystalline field were neglected. The EQQ interaction parameter Γ was determined experimentally. The results from (a) extend the phase diagram to low para concentrations and show that the transition from the hcp to the cubic phase does not take place below $c=0.55$. The data from thermal cyclings, when analyzed in conjunction with corresponding data from x-ray diffraction, indicate that the changes in pressure (and in other thermodynamic properties) are due mainly to the order-disorder transition of the rotational motions and not to the crystalline phase change *per se*. The results from (b) give values of $\Gamma_{\text{eff (pair)}}/k_B = 1.05\pm0.07$ K and $\Gamma_{\text{eff } (c=1)}/k_B = 0.93\pm0.05$ K for low and high concentrations of p-D_2, respectively. For a rigid lattice, the theoretical value is $\Gamma_0/k_B = 1.20$ K. A comparison is made with values of Γ/k_B from a previous determination and with those predicted by the theory of Harris, which takes into account quantum effects in the solid. Anomalies in $(\partial P/\partial T)_V$ at very low p-D_2 concentrations are observed, but are not explained. The entropy of the rotational motion of the $J=1$ state is calculated above 0.4 K and is found to approach $R\ln 3$ per mole of p-D_2 for $c \gtrsim 0.6$.

I. INTRODUCTION

OVER the past five years, many theoretical and experimental papers have appeared which have advanced our understanding of the intriguing properties of solid H_2 and D_2. This work is fairly completely referenced in several recent publications.[1–5] Among the many interesting results are those obtained by x-ray diffraction[2] giving the relative stabilities of the crystalline phases both at 4 K and upon cycling through the phase transition, and those obtained by Raman spectroscopy[6] showing the rotational excitation states in orthohydrogen (o-H_2) and paradeuterium (p-D_2) that had been predicted by several authors.[3,7–10]

† Work supported by the National Science Foundation and the U. S. Army Research Office (Durham).

* Present address: Duke Medical Center, Durham, N. C.

[1] K. F. Mucker, P. M. Harris, D. White, and R. A. Erickson, J. Chem. Phys. **49**, 1922 (1968).

[2] A. F. Schuch, R. L. Mills, and D. A. Depatie, Phys. Rev. **165**, 1032 (1968).

[3] J. C. Raich and R. D. Etters, Phys. Rev. **168**, 425 (1968).

[4] J. F. Jarvis, H. Meyer, and D. Ramm, Phys. Rev. **178**, 1461 (1969).

[5] A. B. Harris, Int. J. Quantum Chem. **IIs**, 347 (1968); and (unpublished).

[6] W. Hardy, I. F. Silvera, and J. McTague, Phys. Rev. Letters **22**, 110 (1969).

[7] S. Homma, K. Okada, and H. Matsuda, Progr. Theoret. Phys. (Kyoto) **38**, 767 (1967).

[8] H. Ueyama and T. Matsubara, Progr. Theoret. Phys. (Kyoto) **38**, 784 (1967).

[9] F. G. Mertens, W. Biem, and H. Hahn, Z. Physik **213**, 33 (1968).

[10] F. G. Mertens, W. Biem, and H. Hahn, Z. Physik **220**, 1 (1969).